JOURNAL OF CATALYSIS 79, 410–419 (1983)

Mechanism of the Alkali Azide Melt Decomposition on Metal Surfaces

H. C. EGGHART

U.S. Army Mobility Equipment Research and Development Command, Countermine Laboratory, Fort Belvoir, Virginia 22060

Received July 6, 1981; revised October 29, 1982

The decomposition of molten KN_3 and CsN_3 catalyzed by surfaces of the group VIII and 1B metals was investigated. These catalytic decomposition reactions followed zero-order kinetics and the activities of the catalysts decreased in the direction from the $VIII_1$ over the $VIII_2$ and $VIII_3$ to the 1B metals. For comparison, the thermal decomposition of transition metal azido complexes in molten salt solutions was studied. These complexes decomposed in first-order reactions and the activation energies of their decomposition reactions followed the same trends as observed in the catalytic decomposition of molten alkali azides on surfaces of the respective metals. These results support the theory that azido species are formed on the metal catalyst surfaces which are related to the respective transition metal azido complexes studied in solution.

INTRODUCTION

At elevated temperatures, inorganic azides decompose according to $2MN_3 \rightarrow 2M + 3N_2$, forming metal and nitrogen. With heavy metal azides, this reaction is highly exothermic, which is a prerequisite for being an explosive. The azides of potassium, rubidium and cesium, however, decompose in slightly endothermic reactions since much energy is required to reduce the alkali metal ions to alkali metals (*1, 2*). These three alkali azides melt before decomposition takes place and their melts decompose very little at temperatures below 450°C. Activation energies of about 50 kcal/mole are required (*3, 4*). In contrast, high rates of decomposition were found in the presence of the metals iron, cobalt, and nickel (*4*). These observations resulted in the investigation of the thermal decomposition of molten KN_3 and CsN_3 on surfaces of all group VIII and 1B metals, presented in this paper.

In view of the high catalytic activity of transition metals for the alkali azide melt decomposition, it was noteworthy that transition metal azides have the lowest thermal stabilities of all inorganic azides. This consideration led to the decision to study the thermal decomposition of a series of analogous transition metal azido complexes in molten salt solutions and to compare the results with the data of the alkali azide melt decomposition, catalyzed by the respective transition metals. By studying the decomposition of the complexes in solution, the complicating influences of the solid state were avoided and it could be expected that the decomposition rates would reflect in a relatively consistent manner the facility with which the primary decomposition step takes place, namely, the excitation and transfer of an electron from the azide ion to the cation of the decomposing species (*1, 2*). Transition metal monoazido complexes in solution in molten alkali nitrates and molten potassium thiocyanate proved useful for this study.

METHODS

1. Apparatus

The kinetics of all decomposition reactions was investigated by measuring the pressure increase resulting from the azide decomposition in a closed vacuum system. For this purpose a high-vacuum glass appa-

0021-9517/83/020410-10$03.00/0

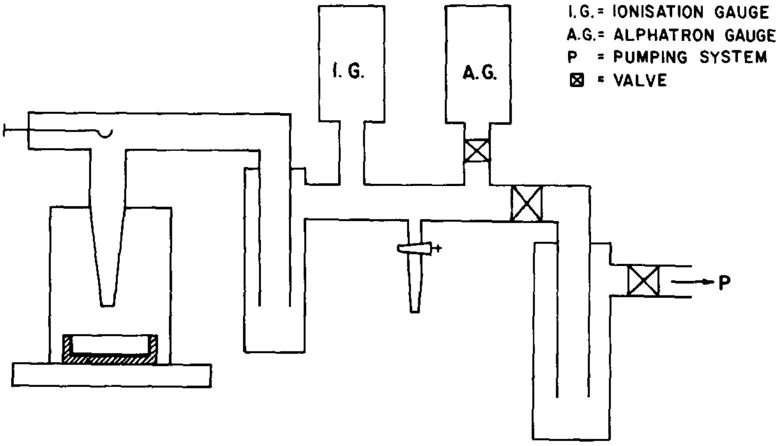

FIG. 1. Schematic representation of the decomposition apparatus.

ratus was built, which is schematically shown in Fig. 1. It permitted a vacuum of better than 10^{-6} Torr. By turning a glass spoon attached to a ground joint it was possible to drop the samples into the reaction vessel of the high-vacuum apparatus. The reaction vessel was surrounded by a heated brass block whose temperature was kept constant electronically. For measuring the change of pressure due to sample decomposition an Alphatron Gauge was used. A recorder, not shown in Fig. 1, recorded the pressure increase as a function of time, i.e., the recorder provided plots of the decomposition curves. The azide sample sizes were chosen to permit the use of the Alphatron Gauge range of 0–100 mTorr. The outgassing rates of the samples and of the apparatus were negligible at these pressures. The decomposition apparatus included two cold traps. One was part of the system in which the nitrogen accumulated during decomposition; the other separated this system from the pumps. All experiments were conducted at temperatures above the melting points of the samples. The volume of the decomposition apparatus was determined by measuring with the Alphatron Gauge the pressure attained when air contained in flasks of calibrated volume was allowed to expand into the evacuated apparatus.

2. Investigation of the Catalytic Decomposition of Molten Alkali Azides

The samples were prepared by mixing metal powders with KN_3 or CsN_3 in exactly known proportions using a vibrating mixer mill. The specific surfaces of these metal powders were determined with the BET method. For performing a decomposition experiment a small pellet consisting of a homogeneous azide/metal powder mixture was placed on a rotatable spoon of the decomposition apparatus. After pumping the air out, the sample and apparatus were outgassed at high-vacuum conditions. This was followed by closing a valve to establish a closed system, which was then checked with the Alphatron Gauge for zero pressure increase in the range 0–10 mTorr. Subsequently, the sample was dropped into the reaction vessel and the decomposition curves were recorded. Melting occurred, due to the very small size of the samples, almost instantaneously after the samples arrived at the bottom of the reaction vessel. The decomposition experiments were conducted at temperatures between 350 and 380°C with the group VIII metals as catalysts and between 400 and 440°C with the 1B metals. At the temperatures used in the catalytic azide decomposition studies the rate of the noncatalytic decomposition was negligible.

The decomposition curves provided by the recorder could be mathematically transformed and expressed as fractional decomposition versus time. This made it possible to compare all decomposition experiments conducted with samples having the same azide/catalyst mixture even when the sample quantities were not the same. Decomposition curves expressed in these terms are shown in Fig. 2. This figure shows, as will be discussed in more detail below, that the catalytic alkali azide melt decompositions take place with essentially constant rates. The temperature dependence of the rates as measured in the constant rate region was used for the determination of the activation energies and frequency factors via the Arrhenius equation. The azide and catalyst quantities and the quantities of nitrogen evolved in each experiment, as well as the specific surfaces of the catalysts, were known; thus the decomposition rates could be expressed as azide molecules decomposed per square centimeter and second.

Another experimental procedure for studying the catalytic azide melt decomposition involved placing the metal powder catalysts into the reaction vessel and initiating the decomposition experiments, after the outgassing period, by dropping a pure alkali azide sample on the catalyst. When this technique was used, the metal powders could be hydrogen treated, *in situ*, at elevated temperatures to assure surface oxide-free catalysts. This could be accomplished by admitting pure hydrogen into the evacuated decomposition apparatus and, after the appropriate treatment times, pumping the hydrogen out. Thus surface oxide-free metal powders could be prepared *in situ* and their properties as catalysts could be investigated without ever again exposing the hydrogen treated metal surfaces to air.

In addition to the experimental procedures described above, the so-called split run technique was used to check the results obtained with the techniques discussed above. This method allows the determination of the decomposition rates at different temperatures of one and the same sample. In the application of this technique to the

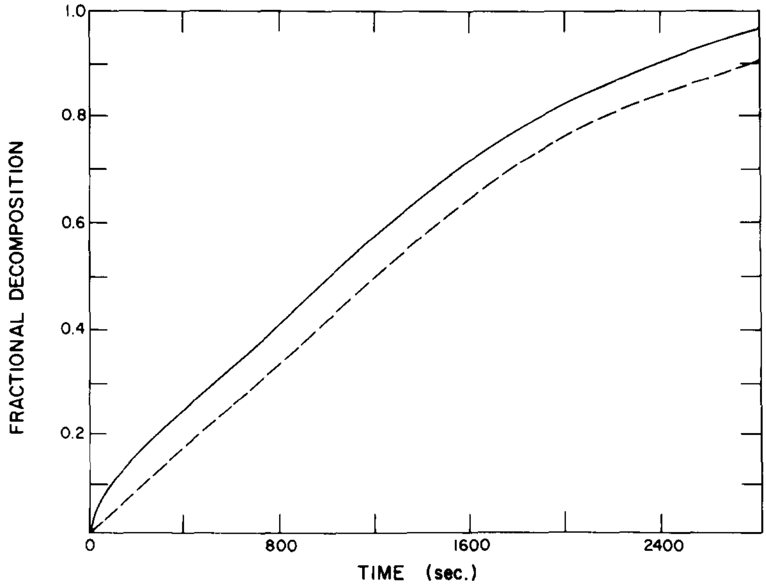

FIG. 2. Decomposition of molten KN_3 at 360°C catalyzed by iron powder. Solid line: catalyst used the first time. Broken line: catalyst used repeatedly or catalyst freed of surface oxide layer by *in situ* hydrogen treatment.

case considered here numerous decompositions could be performed with one sample without leaving the constant rate decomposition region. This was accomplished by using larger samples and decomposing them at lower rates which could be achieved by proper choice of temperatures and catalyst quantities. For sensitivity at low decomposition rates the most sensitive range of the Alphatron Gauge (0–10 mTorr) could be used. After each decomposition run the heated brass block was lowered to stop the decomposition completely. When the brass block had reached the next selected, constant temperature it was raised to the operating position surrounding the reaction vessel. A constant decomposition rate was attained soon thereafter and recorded.

Regardless of the technique used, the data required for the calculation of the Arrhenius parameters were obtained by performing at least 20, and sometimes 40, decomposition experiments at different temperatures. All techniques led to consistent results and the activation energies could be determined with a reproducibility of better than ±1 kcal/mole with the group VIII metals and better than ±2 kcal/mole with the group 1B metals.

3. Investigation of the Transition Metal Monoazido Complexes in Molten Salt Solutions

A. Spectrophotometric studies. The molten eutectic mixture of KNO_3 and $LiNO_3$ (mp 129°C) as well as molten KCNS were the media used in these investigations. The formation of the azido complexes was studied spectrophotometrically at 150°C with the $KNO_3/LiNO_3$ melt and at 185°C with the KCNS melt using a Cary 14 spectrophotometer, optical quartz cells, and a high-temperature sample cell holder. For the preparation of the samples, reagent-grade solvent salts were dried at 110°C overnight, subjected to a shock drying technique involving heating and freezing cycles under vacuum, and weighed and melted under vacuum (*5*). Water-free transition metal salts and potassium azide were added to the melts and portions of the resulting solutions were transferred into the optical quartz cell which was held at the desired temperature by the temperature-controlled sample cell holder. An alternate technique involved adding the transition metal salt and potassium azide to the solvent melt in the optical cell. In this case, a homogeneous mixture was obtained by stirring the melt with a glass fiber.

B. Transition metal monoazido complex decomposition studies. The decomposition of such complexes in molten salt solutions was studied with the decomposition apparatus described above. The samples were prepared by mixing known quantities of water-free transition metal salts, potassium azide, and the above-mentioned dried, solid solvent salts within a little agate vial of a vibrating mixer mill. When dropping a small, outgassed pellet of such a sample into the reaction vessel of the high-vacuum apparatus, almost instantaneous melting and onset of the decomposition reaction occurred. Depending on the temperature chosen, the times required for the decomposition of the azido species in the melt droplet formed ranged from a few minutes to hours. All the transition metal monoazido complexes studied decomposed in perfect first-order reactions. The first-order rate constants of these decompositions were determined at various temperatures and used for the determination of the Arrhenius parameters. The data allowed the determination of the activation energies with a reproducibility of ±1 kcal/mole in the case of the group VIII metal azido complexes and ±1.5 kcal/mole with the Cu(II) azido complex. In the absence of transition metal ions no decomposition was observable at the temperatures of these experiments.

RESULTS

1. Transition Metal-Catalyzed Alkali Azide Melt Decomposition

The transition metal-catalyzed alkali azide melt decomposition resulted in the formation of pure nitrogen, as confirmed mass spectrometrically, and alkali metal. The latter evaporated and condensed as a mirror on the cool, upper part of the reaction vessel. The decomposition reactions on surfaces of all metal catalysts took place with perfectly constant rates from the beginning of each experiment to a fractional decomposition of at least 0.65 if the metal catalysts had been rendered surface oxide-free by a prior, *in situ* hydrogen treatment. An example can be seen in Fig. 2. Above fractional decomposition 0.65, a very gradual decrease of the decomposition rates took place, which is explained by the observation that part of the catalyst powder particles lose contact with the melt droplet when it shrinks due to its decomposition. When a metal powder was used as catalyst which was not freed of surface oxide, an initial, short period of higher decomposition rate was found, followed by the constant rate, as observed with the oxide-free metal catalysts. Perfectly constant rates, however, from the beginning of each experiment to at least 65% fractional decomposition were found with all metal powders when used repeatedly as catalysts without exposing them to air again. This could be accomplished by dropping pure alkali azide samples on the catalyst which remained in the reaction vessel at the end of a decomposition experiment, using one of the three rotatable spoons located within the decomposition apparatus above the reaction vessel. (For simplicity only one spoon is shown in Fig. 1.) Figure 2 shows characteristic decomposition curves as discussed above. The solid line is the decomposition curve of molten KN_3 on iron powder surfaces. Very similar curves were obtained with all group VIII transition metals as catalysts. The broken line is the decomposition curve obtained when the iron powder or any other metal powder was used repeatedly as catalyst without being exposed to air. The broken curve is also an example of the decomposition curves observed with *in situ* hydrogen-treated iron or any other *in situ* hydrogen-treated metal as catalyst. In the decomposition of CsN_3 melts on transition metal powders exactly the same decomposition curves were obtained as shown in Fig. 2 for the catalytic decomposition of KN_3 melts. All these results indicate that the decompositions of molten alkali azides on transition metal surfaces follow essentially zero-order kinetics. More accurately, the decompositions proceed with essentially constant rates, which is not surprising since the reaction products disappear from the liquid phase and the alkali azide concentration in the liquid phase does not change.

In order to better understand the influence of the surface oxide layers, alkali azide melt decompositions in the presence of transition metal oxides were performed. In the presence of oxides such as Fe_3O_4, Co_2O_3, or NiO the decomposition rates were nearly zero during the first 10 sec after initiation of an experiment. This contrasts sharply with the transition metal-catalyzed alkali azide melt decompositions, where the decomposition commences immediately after the sample is dropped into the reaction vessel. After these induction periods, lasting approximately 10 sec, the decomposition rates increased in an acceleratory manner. The lengths of the acceleratory periods, i.e., the fractions of the azide samples decomposed during the acceleratory periods, were directly proportional to the metal oxide-to-azide ratio of the samples. The acceleratory periods were followed by the characteristic decomposition curve of the metal-catalyzed alkali azide melt decomposition. These observations indicated that the oxides themselves exert little or no catalytic effect and that the catalysts were formed during the acceleratory periods. On the basis of thermodynamic considerations reduction of the respective oxides to the metals could be expected. This was unequivocally confirmed by X-ray analysis of decomposition residues. Thus, during the acceleratory periods the oxides are reduced to the respective metals. This reaction is at first very slow but the metals formed catalyze the alkali azide decomposition which results in progressively faster oxide reduction rates until all oxide is reduced. This autocatalytic process results in the induction and acceleratory periods mentioned above. The acceleratory periods are followed by the alkali azide melt decomposition catalyzed by the metals formed. It was shown in these studies with oxides that the metals formed in the acceleratory periods catalyzed the alkali azide melt decomposition with the same activation energies as the metal powders.

In the case of alkali azide melt decomposition on transition metal powders the quantity of surface oxide present is too small for the acceleratory periods to be seen. They could be observed, however, when strongly oxidized metal powders were intentionally used as catalysts. The higher rates in the initial phase of the metal-catalyzed decomposition (solid line in Fig. 2) should not be confused with the acceleratory periods mentioned above. This initial decomposition phase, prior to attaining the constant rate, is due to catalytic decomposition on metal surfaces which briefly before were freed of the oxide layer and had not reached an equilibrium state. The activation energies were the same regardless of whether the rates were obtained from the initial decomposition phase or from the constant-rate region.

It is noteworthy that transition metal ions, introduced into alkali azide melts in the form of transition metal salts, are nearly instantaneously reduced to the respective metals. The metal particles formed in this manner also catalyze the alkali azide melt decomposition as observed with the metal powders (*6*). It is obvious, therefore, that any homogeneous catalysis effects cannot possibly contribute to the heterogeneously catalyzed reaction discussed in this paper.

The recordograms representing the pressure increase in the decomposition apparatus as a function of time constitute the primary experimental data of this work. More than 1000 decomposition experiments were conducted. In view of the large quantity of data collected it does not seem worthwhile to tabulate them. The data permitted, as mentioned under Methods, the determination of the decomposition rates with different catalysts at various temperatures and their expression in terms of azide molecules decomposed per square centimeter and second. The results were double-checked with the split run technique and in the experiments with *in situ* hydrogen-treated metal powders. These rates served for the calculation of the activation energies and frequency factors shown in Table 1. The activation energies of this table could be determined with a reproducibility of better than ±1 kcal/mole with the group VIII metals and better than ±2 kcal/mole with the 1B metals. The frequency factors for silver and gold catalysts are not listed because no accurate data for the specific surfaces of the silver and gold powders were available. The results displayed in Table 1 will be discussed below.

2. Transition Metal Azido Complex Decompositions in Molten Salt Solutions

When the azide ion concentrations in the molten salt solutions were higher than the transition metal ion concentrations, azido complexes formed which decomposed too rapidly to be studied with the techniques used. On the other hand, the complexes formed when the transition metal ion concentrations were higher than the azide ion concentrations decomposed in comparatively slow, first-order reactions. At temperatures near the melting points of the solvent salts, such solutions were thermally stable and were studied spectrophotometrically. The shifts of the ligand field bands and the appearance of charge transfer bands established that azide coordination took place. The comparison of these spectra with the spectra of azido complexes in aqueous solutions showed that the slow-

TABLE 1

Arrhenius Parameters of the KN_3 and CsN_3 Melt Decompositions on Group VIII and 1B Metal Surfaces

	$VIII_1$	$VIII_2$	$VIII_3$	1B
KN_3				
	Fe	Co	Ni	Cu
E_a (kcal. $mole^{-1}$)	31	29	31	41
A (molecules cm^{-2} sec^{-1})	2.9×10^{26}	7.2×10^{25}	3.8×10^{25}	5.0×10^{28}
	Ru	Rh	Pd	Ag
E_a (kcal. $mole^{-1}$)	27	26	33	42
A (molecules cm^{-2} sec^{-1})	4.9×10^{25}	5.4×10^{24}	7.8×10^{24}	
	Os	Ir	Pt	Au
E_a (kcal. $mole^{-1}$)	33	32	34	41
A (molecules cm^{-2} sec^{-1})	4.4×10^{25}	3.0×10^{25}	9.7×10^{25}	
CsN_3				
	Fe	Co	Ni	Cu
E_a (kcal. $mole^{-1}$)	30	28	31	42
A (molecules cm^{-2} sec^{-1})	1.0×10^{26}	6.6×10^{24}	1.1×10^{25}	4.0×10^{27}
	Ru	Rh	Pd	Ag
E_a (kcal. $mole^{-1}$)	28	25	32	42
A (molecules cm^{-2} sec^{-1})	1.9×10^{25}	6.4×10^{23}	2.1×10^{24}	

decomposing species were transition metal monoazido complexes (*7–9*). These complexes were suitable for the purpose of this study, which was to determine the thermal stabilities and decomposition kinetics parameters of a series of analogous transition metal azido complexes and to compare the results with the data obtained in the transition metal-catalyzed alkali azide melt decomposition. The first-order rate constants of the transition metal azido complex decompositions were determined at various temperatures and these rates were used for the calculation of the Arrhenius parameters. The data permitted a reproducibility of the activation energies of better than ±1 kcal/mole in the case of the group VIII metal monoazido complexes and ±1.5 kcal/mole with the Cu(II) monoazido complex. The results for the monoazido complexes of Co(II), Ni(II), Cu(II), Rh(III), and Ir(III) are displayed in Table 2. They will be discussed below. The complexes of the remaining group VIII and 1B ions could not be investigated because they were either thermally too unstable or the respective transition metal ions did not dissolve in the molten salt solvents.

DISCUSSION

The data displayed in Table 1 show that molten KN_3 and CsN_3 decompose, considering the experimental error, with the same activation energy when the same metal catalyst is present. This result lends support to the concept that the alkali metal cations are not involved in the rate-determining step of the transition metal-catalyzed alkali azide melt decomposition. The data of this table also show that the frequency factors are consistently smaller in the catalytic CsN_3 melt decomposition than in the catalytic KN_3 melt decomposition. The smaller frequency factors found with the CsN_3 melt may be due to the larger size of cesium ion which will occupy more catalyst surface area than the potassium ion. Smaller coverages with cesium than with potassium or sodium were reported by investigators who studied the alkali metal adsorption on tran-

TABLE 2

Arrhenius Parameters of the Transition Metal Monoazido Complex Decompositions in Molten KCNS and $KNO_3/LiNO_3$ Solutions

	VIII$_2$	VIII$_3$	
	KCNS		
	Co(II)	Ni(II)	
E_a (kcal. mole^{-1})	35	38	
A (sec^{-1})	2.0×10^{11}	1.7×10^{13}	
	Rh(III)	Pd(II)	
E_a (kcal. mole^{-1})	28	32	
A (sec^{-1})	3.2×10^{10}	4.6×10^{12}	
	Ir(III)		
E_a (kcal. mole^{-1})	29		
A (sec^{-1})	1.2×10^{10}		
	$KNO_3/LiNO_3$		
	Co(II)	Ni(II)	Cu(II)
E_a (kcal. mole^{-1})	35	38	39
A (sec^{-1})	1.5×10^{15}	6.2×10^{13}	4.9×10^{15}

sition metal surfaces using the LEED technique (*10*).

Comparing the Arrhenius parameters of Table 1, i.e., the catalytic activities of the transition metals for alkali azide decomposition, very distinct trends can be recognized. (1) The lowest activation energies are found with the VIII$_2$ metals. (2) With the VIII$_1$ metals the activation energies are somewhat higher but the larger frequency factors more than compensate for this, which results in the highest specific decomposition rates observed. (3) The VIII$_3$ metals are less active catalysts than the other group VIII metals because the activation energies are somewhat higher and the frequency factors do not compensate. (4) The highest activation energies are observed with the 1B metals. With these metals as catalysts very low decomposition rates are found even though a strong compensation effect is operative as the results with copper indicate. Certain trends can be noticed also in the horizontal direction of Table 1. Except for palladium, the activation energies are lowest and the specific rates highest in the second period of the group VIII metals, followed by the metals of the first and third period.

Assuming a surface site density of 10^{15} sites per cm^2 it was possible to express the frequency factors of Table 1 in terms of frequency factors per site and second. The results showed that the frequency factors per site obtained with the VIII$_2$ metals correspond closely to the frequency factors of the VIII$_2$ transition metal monoazido complex decompositions in the KCNS melt (Table 2), while the frequency factors per site of the VIII$_3$ metals do not correspond closely to the frequency factors of the respective VIII$_3$ transition metal monoazido decompositions in the KCNS melt. It does not seem appropriate, however, to attach too much significance to these results, because close examination of Table 2 reveals that the frequency factors of the transition metal monoazido complex decompositions are, in contrast to the activation energies, affected by the solvent melt.

Let us now discuss Table 2 in more detail. The data of this table show that the transition metal monoazido complexes decompose with the same activation energies in both solvent melt systems, i.e., the activation energies are not influenced by the solvent melt ligands. This is an important result indicating that only the azide ion and the transition metal ions are involved in the rate-determining step and that solvent ligands play a secondary role only. Table 2 also shows that the activation energies of decomposition increase in the direction from the left to the right side of the periodic table of elements. Interestingly, this trend in the activation energies parallels the trend of the thermodynamic stabilities of transition metal complexes widely referred to as the natural order of stabilities. This trend was discussed in considerable detail by Irwin and Williams and interpreted in terms of the effective electronegativities of the ions involved and is also frequently attributed to the effects of the ionic radii of the cations and the superimposed contributions of the crystal-field stabilization energies (*11–13*). The frequency factors of Table 2 indicate that the transition metal complexes decompose in KCNS melt solution with low or near normal first-order rate constants (negative entropies of activation) and in the alkali nitrate melt solution with high or near normal first-order rate constants (positive entropies of activation).

Comparing the data of Tables 1 and 2, similarities in the trends of the activation energies are found which are of particular interest within the framework of this investigation. The $VIII_1$ transition metal monoazido complexes are not listed in Table 2 because they were thermally too unstable to be studied. This is interesting in view of the observation that the use of $VIII_1$ metals as catalysts for alkali azide melt decomposition resulted in the highest decomposition rates observed. The $VIII_2$ metal monoazido complexes decomposed with the lowest activation energies as did alkali azide melts on $VIII_2$ metal catalysts. As in the catalytic decomposition, the activation energies increased and the rates decreased in the direction from the $VIII_2$ over the $VIII_3$ to the 1B metal complexes. Comparing the different periods represented in Table 2, it can be seen that the activation energies are lowest in the second period, a trend also found in the catalytic alkali azide melt decompositions on the respective metal surfaces.

If only the data of Table 1 were available one could be led to interpret the results on the basis of the collective electronic properties of metals using the electron band theory or Pauling's valence bond theory of metals (*14, 15*). The significant difference in the catalytic activities of group VIII and 1B metals would be viewed as a consequence of the partially filled *d*-band or the partially filled atomic *d*-orbitals, respectively. If one considers, however, the results of the transition metal monoazido complex decompositions (Table 2) in addition to the catalysis work (Table 1) one realizes that the above interpretation is not appropriate. It seems unlikely that the similarities in the trends of the activation energies of the catalytic alkali azide melt decompositions and of the transition metal monoazido complex decompositions are coincidental. They suggest a related mechanism of the heterogeneous and homogeneous decompositions, i.e., they suggest that the azide ions become adsorbed on the surfaces of the transition metal catalysts whereby a surface azide species is formed which is related to the respective transition metal monoazido complex in solution. Both the activation energies for the decomposition of these surfaces azide species and the activation energies for the decomposition of the transition metal azido complexes in solution appear to be affected by the thermodynamic stabilities as expected on the basis of the "natural order of stabilities" of transition metal complexes.

The results of this paper are consistent with a mechanism of the alkali azide melt decomposition on surfaces of transition metal catalysts as follows: When an azide ion comes into contact with the metal surface it will become adsorbed whereby a positive charge may become localized at the adsorption site. A surface azide entity will thus be formed which is related to the respective transition metal monoazido complex as studied in the molten salt solutions. The alkali metal ions will also tend to adsorb on the transition metal surface whereby a negative charge will become localized at the adsorption site resulting in binding by the image force as discussed by DeBoer (*16*). When sufficient thermal energy is supplied to the adsorbed azide ion it will transfer an electron to the transition metal surface atom which was partially "demetallized" by the azide ion adsorption. The data of this investigation suggest that this step of the decomposition reaction is rate determining as is the case in azide decomposition in general (*1, 2*). The azide radical thus formed on the catalyst surface will tend to interact with an azide radical formed on an adjacent site because monomolecular decomposition of azide radicals is forbidden by the correlation (spin conservation) rules (*1, 2*). The energy released in the resulting formation of three molecules of nitrogen provides the driving force for the electron transfer from the catalyst to the adsorbed alkali metal ion. Evaporation of the alkali metal follows. In this mechanism the transition metal catalysts provide an energetically more favorable path for the alkali azide decomposition than possible in the usual alkali azide melt decomposition mechanism where direct electron transfer to the alkali metal ions must take place. A mechanism involving the adsorption of two azide ions to one transition metal surface atom, i.e., the formation of an actual transition metal azide, is not as probable as the mechanism discussed above because such species would decompose with much smaller activation energies than were observed in this work. The catalytic mechanism proposed above may seem complicated but it is not. It involves the decomposition of a transition metal azido species formed on the catalyst surface accompanied by electron transfer, via the catalyst, from the azide ion to the adsorbed alkali metal ion.

In this work an unconventional catalytic system was investigated which is distinguished by simplicity. It offered the advantage that the reactions of azides are simple and were widely investigated in the past. Furthermore, the mechanism of azide decompositions is comparatively well understood. The results of this work represent an interesting example for the relationship between heterogeneous and homogeneous reactions.

REFERENCES

1. Evans, B. L., Yoffe, A. D., and Gray, P., *Chem. Rev.* **4,** 515 (1959).
2. Yoffe, A. D., "Development in Inorganic Nitrogen Chemistry" (C. B. Colburn, Ed.), Vol. 1, Chap. 2, p. 72. Elsevier, Amsterdam/London/New York, 1966.
3. Jacobs, P. W. M., and Tompkins, F. C., *Proc. Roy. Soc. London Ser. A* **215,** 265 (1952).
4. Egghart, H. C., *Inorg. Chem.* **2,** 364 (1963).
5. Rhodes, E., and Ubbelohde, A. R., *Proc. Roy. Soc. London Ser. A* **251,** 156 (1959).
6. Egghart, H. C., *Inorg. Chem.* **4,** 1196 (1965).
7. El-Shamy, H. K., and Nassar, M. P., *J. Inorg. Nucl. Chem.* **16,** 124 (1960).
8. Egghart, H. C., *J. Inorg. Nucl. Chem.* **31,** 1538 (1969).
9. Egghart, H. C., *J. Inorg. Nucl. Chem.* **43,** 1390 (1981).
10. Gerlach, R. L., and Rhodin, T. N., *Surf. Sci.* **17,** 32 (1969).
11. Irving, H., and Williams, R. J. P., *J. Chem. Soc.,* 3192, October 1953.
12. Holmes, O. G., and McClure, D. S., *J. Chem. Phys.* **26,** 1686 (1957).
13. Basolo, F., and Rearson, G. R., "Mechanism of Inorganic Reactions." Wiley, New York/London/Sydney, 1968.
14. Mott, N. F., and Jones, H., "The Theory of the Properties of Metals and Alloys." Oxford Univ. Press, New York/London, 1936.
15. Pauling, L., *Proc. Roy. Soc. London Ser. A* **196,** 343 (1949).
16. DeBoer, J. H., "Advances in Catalysis and Related Subjects," Vol. 8, p. 17. Academic Press, New York, 1956.